atmosphere

MDPI

Article

Effects of Nitrogen Rate and Fertilizer Type on Gaseous Nitrogen Losses and Soil Nitrogen Storage in Alkaline Maize Fields of the Hetao Irrigation District

Yu Gao [1,2,3], Yunfei Di [1,2], Haibo Yang [1,2], Yuzhe Tang [1,2], Weijian Zhang [1,2], Yuncai Hu [4] and Fei Li [1,2,*]

[1] College of Resources and Environment, Inner Mongolia Agricultural University, Hohhot 010011, China; gaoyu6670@163.com (Y.G.); diyunfei@emails.imau.edu.cn (Y.D.); haiboyang@imau.edu.cn (H.Y.); tangyuzhe9702@163.com (Y.T.); zhangwj1110@126.com (W.Z.)
[2] Inner Mongolia Key Laboratory of Soil Quality and Nutrient Resources, Hohhot 010018, China
[3] Institute of Resources, Environment and Sustainable Development, Inner Mongolia Academy of Agriculture and Animal Husbandry Sciences, Hohhot 010031, China
[4] Department of Life Science Engineering, School of Life Sciences, Technical University of Munich, 85354 Freising, Germany; yc.hu@tum.de
* Correspondence: lifei@imau.edu.cn

Abstract

Gaseous nitrogen losses and residual soil nitrogen accumulation are primary drivers of low nitrogen use efficiency in alkaline irrigated cropping systems. A two-year field experiment (2019–2020) in the Hetao Irrigation District under alkaline flood-irrigated maize evaluated the effects of nitrogen rate, fertilizer formulation, and enhanced-efficiency fertilizers—urea with urease inhibitor NBPT and ammonium sulfate with nitrification inhibitor DMPP—on NH_3 volatilization, N_2O emissions, post-harvest soil mineral nitrogen, and grain yield. A soil pH manipulation sub-experiment (±0.5 units, ambient pH ~8.8) was conducted to quantify the direct effect of alkalinity on volatilization. NH_3 volatilization was insensitive to fertilizer formulation and inhibitor inclusion but strongly responsive to soil pH; a 0.5-unit increase in soil pH elevated volatilization efficiency by up to 25% relative to ambient conditions. N_2O emissions were around 18% higher under ammonium sulfate than under urea and were reduced by 21–32% with inhibitor treatments, without increasing NH_3 volatilization. Inhibitor-assisted optimized management (urea + NBPT and ammonium sulfate + DMPP) achieved higher yields and lower emission intensity than urea alone. These results confirm that NH_3 and N_2O losses are governed by distinct controls, and that concurrent mitigation of both pathways requires interventions that independently target each loss driver, beyond rate optimization and inhibitor application alone.

Keywords: ammonia volatilization; nitrous oxide emissions; soil nitrogen storage; enhanced-efficiency fertilizer; soil pH; maize; Hetao Irrigation district

Check for updates

Academic Editor: László Bencs

Received: 13 April 2026
Revised: 6 May 2026
Accepted: 13 May 2026
Published: 15 May 2026

Copyright: © 2026 by the authors. Licensee MDPI, Basel, Switzerland. This article is an open access article distributed under the terms and conditions of the Creative Commons Attribution (CC BY) license.

1. Introduction

Nitrogen fertilizer has been central to the dramatic increases in global crop production over the past half-century, yet a large fraction of applied nitrogen is not recovered by crops and instead escapes to the environment through gaseous losses—principally as ammonia (NH_3) and nitrous oxide (N_2O) [1,2]. Global agricultural NH_3 emissions have grown rapidly since 1980, and synthetic fertilizers account for an average of 12–18% of the nitrogen applied that is lost as NH_3 [1,2]. Excessive NH_3 deposition drives soil acidification, eutrophication of water bodies, and—through secondary reactions with sulfur oxides and

nitrogen oxides—the formation of fine particulate matter, contributing substantially to regional haze events [3,4]. N_2O is among the most potent anthropogenic greenhouse gases, with a 100-year global warming potential 273 times that of CO_2 [5]; soils contribute more than 80% of total biospheric N_2O flux to the atmosphere [6], and agricultural production accounted for approximately 74% of human-driven N_2O emissions in the 2010s, with direct agricultural emissions reaching 3.9 Tg N yr^{-1} in 2020 [7]. Managing both loss pathways simultaneously is, therefore, a central challenge for sustainable intensification of crop production, yet the contrasting sensitivities of NH_3 volatilization and N_2O emission to the same management inputs mean that interventions designed to reduce one gas frequently have limited or even counterproductive effects on the other [8,9].

Nitrogen application rate is the primary driver of both NH_3 volatilization and N_2O emissions, operating by elevating soil ammonium (NH_4^+) concentrations that simultaneously provide a substrate for both hydrolysis-driven pH increases favorable to NH_3 formation and for nitrification–denitrification processes that produce N_2O [10]. Soil pH exerts a particularly strong additional control on NH_3 volatilization: losses increase sharply above pH 7.5, as the thermodynamic equilibrium between NH_4^+ and NH_3 shifts progressively toward the gaseous form with increasing alkalinity [11]. Enhanced-efficiency fertilizers (EEFs), principally urease inhibitors (UI) such as N-(n-butyl) thiophosphoric triamide (NBPT) and nitrification inhibitors (NI) such as 3,4-dimethylpyrazole phosphate (DMPP), have been widely proposed as tools to reduce gaseous nitrogen losses by slowing urea hydrolysis and suppressing nitrification, respectively. Meta-analyses indicate that NBPT reduces cumulative NH_3 emissions by approximately 52–61% on average [12,13], while DMPP and related NIs reduce N_2O by approximately 49% [14]. However, EEF effectiveness is strongly context-dependent, and the two inhibitor classes address fundamentally different loss pathways: field experiments in intensive maize cropping systems of northern China have demonstrated that the trade-off between NH_3 volatilization and N_2O reduction persists when NIs are applied at the soil surface [9]. Critically, the NI application has been shown to increase NH_3 emissions by an average of 35.7% globally—with this NH_3 penalty positively correlated with soil pH—so that in alkaline soils the trade-off between N_2O reduction and NH_3 amplification becomes particularly pronounced [8]. When indirect NH_3-derived N_2O is accounted for, the net climate benefit of NI application is substantially reduced [8]. Furthermore, a 30-year global synthesis found that DMPP was statistically ineffective for N_2O reduction in alkaline soils, where soil pH and microbial community composition reduced its efficacy [15]. These findings collectively indicate that the partial decoupling of NH_3 and N_2O pathways is not merely a theoretical concern but a quantifiable management reality, particularly under the alkaline soil conditions that characterize large irrigated agricultural regions of northern China.

The Hetao Irrigation District of Inner Mongolia, one of the three largest irrigation districts in China, exemplifies the intersection of these challenges [16]. The district is characterized by alkaline soils (pH typically exceeding 8.0), conventional nitrogen application rates substantially above crop requirements, and seasonal flood irrigation delivering 3600–4500 m^3 ha^{-1} through the Yellow River canal network—conditions under which crop nitrogen use efficiency averages well below 50% [17], leaving a large nitrogen surplus that accumulates in the soil profile or is lost to the environment [18,19]. Residual mineral nitrogen in the soil profile following harvest represents a legacy pool susceptible to subsequent leaching and denitrification losses, and has been shown to reach 453–749 kg N ha^{-1} in the 0–4 m soil profile of wheat and maize croplands across northern China under conventional nitrogen management, representing a substantial reservoir at risk of leaching under future rainfall intensification [20]. Beyond soil nitrogen accumulation, China's agricultural soils have been estimated to contribute approximately 23% of global NH_3 and 20% of global

N_2O emissions from synthetic fertilizer use, with maize among the three leading reactive nitrogen emitters among crop types [21]. Under flood irrigation, the rapid transition from aerobic to anaerobic soil conditions following inundation creates transient reducing environments that intensify denitrification and N_2O production within narrow post-irrigation time windows [22], while the alkaline soil matrix simultaneously sustains high background rates of NH_3 volatilization [11]. The combination of high pH, high nitrogen inputs, and repeated flood irrigation events, therefore, creates a system in which the performance of EEFs and the relative magnitudes of competing nitrogen loss pathways may diverge substantially from predictions based on studies conducted in more neutral, rainfed, or drip-irrigated systems. Despite the agronomic and environmental importance of this region, the trade-offs among gaseous nitrogen losses, residual soil nitrogen accumulation, and crop productivity under different fertilizer management strategies are governed by interactions among nitrogen rate, soil properties, and irrigation-induced anaerobic dynamics that vary substantially across systems and are difficult to predict from models or studies conducted under contrasting conditions [23,24]. Nevertheless, studies that simultaneously quantify cumulative NH_3 volatilization, N_2O emissions, and residual soil mineral nitrogen storage across a range of fertilizer management strategies—including direct assessment of soil pH effects on volatilization and evaluation of inhibitor performance—remain scarce for alkaline flood-irrigated maize production.

To address these gaps, we conducted a two-year field experiment (2019–2020) in the Hetao Irrigation District, comparing the effects of nitrogen application rate, fertilizer form, and enhanced-efficiency fertilizers on NH_3 volatilization, N_2O emissions, post-harvest soil mineral nitrogen storage, and maize grain yield. A soil pH manipulation sub-experiment was embedded within the main trial to directly quantify the contribution of soil alkalinity to NH_3 volatilization efficiency under field conditions. The study addressed three questions: (1) Do nitrogen application rate, fertilizer formulation, and inhibitor inclusion exert differential effects on cumulative NH_3 volatilization and N_2O emissions, and which factors are the primary determinants of each loss pathway under alkaline flood-irrigated conditions? (2) How sensitive is NH_3 volatilization efficiency to soil pH across a controlled gradient under field conditions? And (3) Which fertilizer management strategy most effectively balances the reduction of gaseous nitrogen losses, improvement of greenhouse gas emission intensity, and maintenance of grain yield in this system?

2. Materials and Methods

2.1. Study Site and Experimental Design

The field experiment was conducted at the Yonglian Village Research Base, Wuyuan County, Bayannur City, Inner Mongolia Autonomous Region, China (41°4′ N, 108°2′ E; altitude 1027 m a.s.l.). The site experiences a temperate continental climate with a mean annual temperature of 6.1 °C, a cumulative active temperature (≥10 °C) of 3362.5 °C, and a frost-free period of 117–136 days. Mean annual precipitation is 170 mm, concentrated predominantly in the summer and autumn months. Monthly precipitation and mean air temperature during the two growing seasons are presented in Figure 1. The soil is classified as an Irragric Anthrosol (World Reference Base for Soil Resources, WRB), with a silt loam texture and a bulk density of 1.40 g cm^{-3}. Prior to experimental establishment, the topsoil (0–20 cm) had an organic matter content of 21.64 g kg^{-1}, alkaline-hydrolyzable N of 53.4 mg kg^{-1}, available P of 20.08 mg kg^{-1}, available K of 132.95 mg kg^{-1}, $CaCO_3$ equivalent content of 105.27 g kg^{-1}, CEC of 11.78 cmol(+) kg^{-1}, exchangeable sodium percentage (ESP) of 8.9%, and a pH of 8.8. Soil organic matter was determined by the potassium dichromate oxidation method, alkaline-hydrolyzable N by the alkaline hydrolysis diffusion method, available P by the sodium bicarbonate extraction method (Olsen

method), available K by ammonium acetate extraction, $CaCO_3$ equivalent by the volumetric calcimeter method, CEC by the ammonium acetate method, ESP by calculation from exchangeable sodium and CEC, and pH in a 1:2.5 soil-to-water suspension [25].

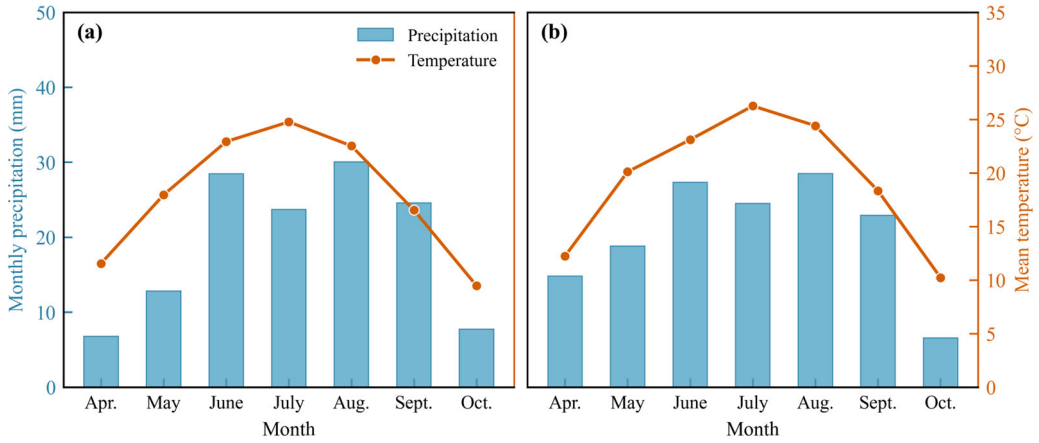

Figure 1. Monthly precipitation and mean air temperature during the growing season in (**a**) 2019 and (**b**) 2020.

A two-year field experiment was conducted during the 2019 and 2020 maize (*Zea mays* L.) growing seasons. The maize variety was Xinyu 12, sowing occurred at the end of April, and harvest occurred in early October in both years. Each experimental plot measured 6.5 m × 10 m. Six treatments were arranged in a randomized complete block design with four replications (Table 1): an unfertilized control (CK); an optimized nitrogen rate applied as urea (OPT-U; 180 kg N ha^{-1}, determined by soil testing and fertilizer recommendation based on pre-experiment soil nutrient analysis and local maize nitrogen demand); a conventional high nitrogen rate applied as urea (CON-U; 400 kg N ha^{-1}, reflecting the mean application rate established through pre-experiment farmer surveys in the local area; urea combined with the urease inhibitor NBPT at the optimized rate (OPT-IU); ammonium sulfate alone at the optimized rate (OPT-AS); and ammonium sulfate combined with the nitrification inhibitor DMPP at the optimized rate (OPT-IAS).

Table 1. Experimental treatment design showing nitrogen application rates and split-application schedule.

Treatment	Fertilizer Form	Basal N (kg ha^{-1})	Topdressing N (kg ha^{-1})	Total N (kg ha^{-1})
CK	—	0	0	0
OPT-U	Urea	54	126	180
CON-U	Urea	120	280	400
OPT-IU	Urea + NBPT	54	126	180
OPT-AS	Ammonium sulfate	54	126	180
OPT-IAS	Ammonium sulfate + DMPP	54	126	180

Nitrogen was applied with 30% as a basal fertilizer and 70% as a topdressing. Basal fertilizer was incorporated into the soil prior to the first irrigation event. Topdressing was applied at the V6 growth stage, followed immediately by flood irrigation. Both inhibitor-treated fertilizers (OPT-IU and OPT-IAS) were commercially available pre-incorporated products: NBPT (N-(n-butyl) thiophosphoric triamide; purity ≥98%, water-soluble powder formulation) was pre-incorporated into urea at a rate of 1% of the fertilizer-N applied (*w*/*w*), and DMPP (3,4-dimethylpyrazole phosphate; purity ≥98%, water-soluble formulation) was pre-incorporated into ammonium sulfate at a rate of 1% of the ammonium-N content (*w*/*w*).

Inhibitor-treated fertilizers were applied following the same split-application schedule as the corresponding non-inhibitor treatments, with no additional handling steps. Phosphorus (90 kg P ha^{-1}) and potassium (120 kg K ha^{-1}) fertilizers were applied uniformly as seed fertilizers in a single basal application across all treatments. Flood irrigation was applied three times per growing season, using water from the Yellow River supplied through the Hetao Irrigation District canal network. Irrigation volumes at crop growth stages V6, R1, and R4 were approximately 1200, 1000, and 1400 m^3 ha^{-1}, respectively, determined by flow meter readings at the branch canal, for a total seasonal irrigation volume of approximately 3600 m^3 ha^{-1}. All other agronomic practices followed local conventional management.

2.2. Soil pH Microplot Experiment

To isolate and directly quantify the effect of soil pH on NH_3 volatilization under field conditions, soil pH manipulation microplots (1.5 m × 0.8 m) were established within each plot of the five fertilized treatments (OPT-U, CON-U, OPT-IU, OPT-AS, and OPT-IAS) across all four replicate blocks. Within each plot, one microplot was adjusted to elevated pH (pH^+) and one to reduced pH (pH^-), yielding four microplots per pH condition per treatment. Soil pH was adjusted in the upper 0–30 cm layer relative to the ambient plot pH (~8.8) by approximately ±0.5 units, yielding elevated (pH^+, ~9.3–9.4) and reduced (pH^-, ~8.3) conditions. Soil pH elevation was achieved by thoroughly mixing 110.16 g of calcium oxide (CaO) dissolved in water with the excavated topsoil; soil pH reduction was achieved by mixing 3.1 L of 0.368 mol L^{-1} sulfuric acid (H_2SO_4) with the excavated soil. Following the amendment, soil pH was analytically verified before backfilling.

The physical disturbance associated with soil excavation and backfilling required approximately 20 days for bulk density to return to values representative of the surrounding plot. Soil pH in each microplot was monitored continuously after adjustment; values converged to ambient plot levels by approximately day 22 post-adjustment and remained stable thereafter. Accordingly, differences in NH_3 volatilization attributable to pH manipulation were detectable only within this ~22-day window. Because the settlement period precluded safe installation of static N_2O flux chambers, pH effects on N_2O emissions were not measured within the microplots and are evaluated only through the main-plot treatment comparisons.

2.3. NH_3 Volatilization Measurement

Ammonia volatilization was quantified using the ventilation (venting) method following the protocol of Wang [26]. Each capture device consisted of a rigid polyvinyl chloride (PVC) tube (inner diameter 15 cm, height 15 cm) fitted with two polyurethane sponges (diameter 16 cm, thickness 2 cm each) pre-soaked in 15 mL of glycerol-phosphate absorption solution (50 mL phosphoric acid and 40 mL glycerol, adjusted to 1000 mL with deionized water). The lower sponge was positioned 5 cm from the tube base; the upper sponge was placed flush with the tube rim (Figure 2). Each device was placed with its base resting on the soil surface, enclosing the measurement area in a cap-like configuration without soil insertion, thereby allowing free gas exchange at the soil–device interface. Three devices were deployed randomly per plot, positioned away from plot borders to avoid inter-plot contamination; the same deployment of three devices was applied within each microplot.

Monitoring commenced on the day following each fertilization event. During the 6-day intensive monitoring window after each fertilization and irrigation event, sampling was conducted every 2 days; during non-intensive periods, frequency was reduced to every 15–25 days. At each interval, sponges were retrieved and extracted with 300 mL of 2 mol L^{-1} KCl solution by oscillation for 1 h, and the NH_3-N concentration in the extract was determined using a continuous-flow analyzer (AA3, Bran + Luebbe GmbH,

Norderstedt, Germany). The NH_3 volatilization rate (N, kg ha^{-1} d^{-1}) and cumulative seasonal losses were calculated by linear interpolation between consecutive sampling dates. NH_3 volatilization efficiency (%) was expressed as the ratio of cumulative NH_3 volatilization to total nitrogen applied.

$$N = \frac{M}{A \times D} \times 10^{-2} \quad (1)$$

$$\text{Cumulative } NH_3 = \sum [N \times D] \quad (2)$$

where M is the mean NH_3-N mass (mg) captured by a single device, A is the cross-sectional area of the capture device (m^2), and D is the interval between successive measurements (d).

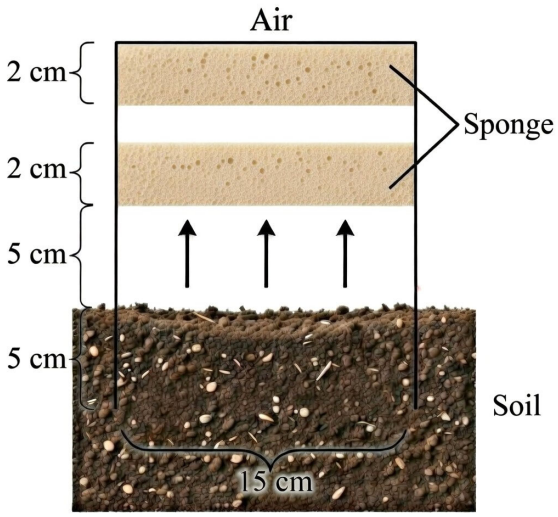

Figure 2. Structure drawing of venting method for NH_3 volatilization.

2.4. N_2O Flux Measurement

Nitrous oxide emission flux was measured using the static closed-chamber method. One chamber system was permanently installed per experimental plot, giving 24 chambers in total (6 treatments × 4 replicates). Each chamber system consisted of a stainless steel box (50 cm × 50 cm × 70 cm, wall thickness 1.2 cm) externally insulated with a foam layer, mounted on a permanently installed stainless steel base frame (50 cm × 50 cm × 15 cm, inserted 12 cm into the soil) fitted with a water-filled sealing channel (Figure 3). A three-way sampling valve and temperature port were positioned ~25 cm above the base frame.

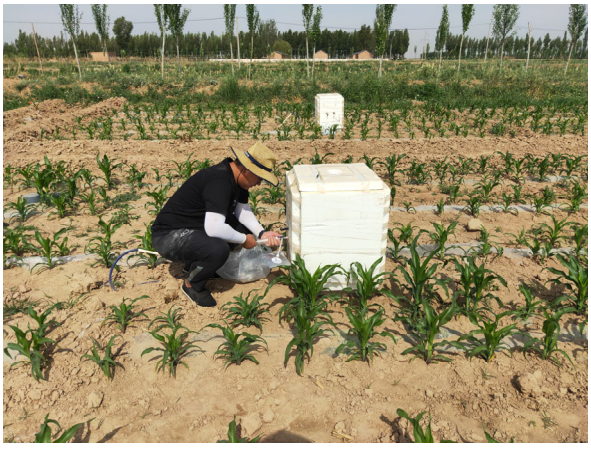

Figure 3. Static dark box used to determine N_2O.

Gas samples were collected at 10-day intervals during the background monitoring period (i.e., all periods outside the post-event intensive windows), increasing to every 2 days during the 7-day period following each fertilization and flood irrigation event, as flood inundation independently generates transient anaerobic conditions that drive significant N_2O pulses. In both years, the growing season extended from late April (sowing) to early October (harvest), approximately 155 days. Intensive sampling was therefore triggered on three occasions: (i) the first flood irrigation combined with topdressing in mid-May; (ii) the second flood irrigation in mid-June; and (iii) the third flood irrigation in early July. All sampling was conducted between 08:30 and 11:30 h local time, a window selected to approximate the daily mean N_2O flux consistent with standard protocols widely adopted in static closed-chamber studies in northern Chinese cropping systems. Sampling was carried out simultaneously by multiple field teams, with chamber closure times staggered across plots to ensure all measurements fell within this window; each plot required approximately 35 min to complete. In total, approximately 24 sampling occasions were conducted per plot per growing season (12 intensive and approximately 12 background occasions), yielding approximately 96 gas samples per plot per season (4 time-point samples × 24 occasions) and approximately 4600 gas samples across all plots and both growing seasons.

Gas samples were withdrawn by syringe at 0, 10, 20, and 30 min after chamber closure and transferred to pre-evacuated vials; N_2O concentrations were determined using a Picarro G2308 cavity ring-down spectroscopy analyzer (Picarro Inc., Santa Clara, CA, USA). Cumulative N_2O emissions were calculated by trapezoidal interpolation between consecutive flux measurements.

The N_2O emission flux (F, μg m^{-2} h^{-1}) was calculated as:

$$F = \rho \times h \times \frac{\Delta c}{\Delta t} \times \frac{273}{273 + T} \quad (3)$$

where ρ is the gas density of N_2O under standard conditions (kg m^{-3}), h is the effective headspace height of the sampling chamber (m), calculated as the total internal chamber height (0.70 m) minus the depth of the base frame inserted into the soil (0.12 m), giving h = 0.58 m; $\Delta c/\Delta t$ is the rate of N_2O concentration change within the chamber (μL L^{-1} h^{-1}), 273 is the absolute temperature at 0 °C (K), and T is the mean air temperature (°C) inside the chamber during sampling. All flux values were converted to daily emission flux units (g ha^{-1} d^{-1}) to facilitate inter-period comparisons.

Cumulative N_2O emissions (g ha^{-1}) were calculated by trapezoidal interpolation between consecutive sampling dates:

$$CE = \sum \left(\frac{F_i + F_{i+1}}{2} \times 10^{-3} \times d \times 24 \times 10 \right) \quad (4)$$

where CE is the cumulative N_2O emission (g ha^{-1}), F_i and F_{i+1} are the emission fluxes at two consecutive sampling times (mg m^{-2} h^{-1}), and d is the number of days between adjacent sampling intervals.

2.5. Post-Harvest Soil Mineral Nitrogen and Profile Nitrogen Storage

To assess the residual soil nitrogen remaining in the soil profile at the end of each growing season, soil samples were collected by depth increment (0–30, 30–60, and 60–90 cm) from each plot immediately following maize harvest in both 2019 and 2020. At each plot, three soil cores were extracted using a soil auger and composited by depth layer to yield one representative sample per layer per plot. Fresh soil subsamples were extracted with 2 mol L^{-1} KCl solution (soil:solution ratio 1:5, w/v) by shaking for 1 h at room temperature, followed by filtration through Whatman No. 42 filter paper. Ammonium

nitrogen (NH_4^+-N) and nitrate nitrogen (NO_3^--N) concentrations in the filtrate were determined colorimetrically using a continuous flow analyzer (AA3, Bran + Luebbe GmbH, Norderstedt, Germany). Extract concentrations (mg L^{-1}) were converted to a soil dry-mass basis (mg kg^{-1}) using the 1:5 extraction ratio prior to calculation of nitrogen storage.

Soil nitrogen storage (S, kg ha^{-1}) within each depth increment was calculated as:

$$S = C \times \rho_b \times d \times 10 \quad (5)$$

where C is the NH_4^+-N or NO_3^--N concentration expressed on a soil dry-mass basis (mg kg^{-1}), ρ_b is the soil bulk density (g cm^{-3}) of the respective layer, and d is the thickness of the soil layer (cm). The factor 10 converts units to kg ha^{-1}. Total profile nitrogen storage (0–90 cm) was obtained by summing the storage values across all three depth increments. Soil bulk density for each layer was determined from undisturbed core samples collected at the beginning of the experiment using the cutting-ring method.

2.6. Maize Grain Yield Measurement

Grain yield was determined at physiological maturity in a representative harvest area of 6.6 m^2 per plot, avoiding border rows. Harvested grain was oven-dried to a constant weight, and yield was expressed as dry matter yield (kg ha^{-1}) adjusted to a standard moisture content of 14%.

2.7. Greenhouse Gas Warming Potential and Emission Intensity

The global warming potential (GWP, kg CO_2-eq ha^{-1}) attributable to N_2O emissions during the crop growing season was calculated as:

$$GWP = 273 \times R_{N_2O} + GWP_{background} \quad (6)$$

where R_{N_2O} is the cumulative N_2O emission during the growing season (kg ha^{-1}), and the factor 273 reflects the 100-year global warming potential of N_2O relative to CO_2 [5]. Background GWP from CH_4 and CO_2 soil respiration was determined from concurrent static chamber flux measurements at the experimental site during the 2019–2020 growing seasons, yielding a site-specific value of 3023 kg CO_2-eq ha^{-1}, which was incorporated into the total GWP calculation for each treatment.

The greenhouse gas emission intensity (GHGI, kg CO_2-eq kg^{-1} grain) was calculated as:

$$\mathrm{GHGI} = \frac{GWP}{\mathrm{Yield}} \quad (7)$$

where Yield is the grain yield (kg ha^{-1}) of maize at harvest.

2.8. Statistical Analysis

All data were compiled in Microsoft Excel 2024. Statistical analyses were performed in SPSS Statistics v30.0 (IBM Corporation, Armonk, NY, USA). Figures were produced using Python 3.13 with the Matplotlib library (v3.10.6). Each treatment was replicated in four independent blocks (n = 4); sub-plot measurements within each plot—three NH_3 capture devices and three composited soil cores per depth increment—were averaged to yield a single plot-level value prior to analysis, so that the plot mean constituted the unit of replication throughout. Because year represented a confounded climatic and pedological covariate rather than a controlled experimental factor, one-way ANOVA was conducted independently for each growing season, with treatment as the sole factor; cross-year robustness of treatment effects was evaluated by the consistency of treatment rank orders and significance patterns across both years. Differences among treatment

means for cumulative NH_3 volatilization, cumulative N_2O emissions, post-harvest soil mineral nitrogen storage, GWP, GHGI, and grain yield were evaluated using one-way ANOVA for each year separately, followed by Duncan's multiple-range test for post-hoc pairwise comparisons ($p < 0.05$). To evaluate the effects of fertilizer treatment and soil pH manipulation on NH_3 volatilization efficiency, a two-way mixed ANOVA was performed for each year separately, with Treatment as the between-subject factor and pH condition (pH^-, ambient, pH^+) as the within-subject factor, using block as the subject unit. To evaluate the effect of growth stage on cumulative NH_3 volatilization and N_2O emissions, one-way ANOVA was performed with growth stage (Period 1, Period 2, and Period 3) as the independent variable across all treatments for each year separately. The significance threshold was set at $p < 0.05$. Pearson correlation coefficients were computed among nitrogen application rate, cumulative NH_3 volatilization, cumulative N_2O emissions, post-harvest soil nitrogen storage, and grain yield using plot-level observations pooled across both years ($n = 48$). Ninety-five percent confidence intervals for each correlation coefficient were calculated using the Fisher z-transformation. To assess interannual stability, correlations were additionally computed separately for each growing season ($n = 24$ per year). Significance was assessed at $p < 0.05$ and $p < 0.01$.

3. Results

3.1. NH_3 Volatilization and Soil pH Effects

Nitrogen application rate was the primary factor associated with cumulative NH_3 volatilization, with CON-U producing significantly greater seasonal losses than all optimized-rate treatments in both years ($p < 0.05$), while the unfertilized CK lost less than 7 kg ha^{-1} in either year (Figure 4). Among optimized-rate treatments, neither fertilizer formulation nor inhibitor inclusion resulted in significant differences in cumulative emissions in either year ($p > 0.05$), although OPT-AS exceeded OPT-U by 6.4% in 2020. Period 2 consistently accounted for the largest share of seasonal NH_3 loss across fertilized treatments (41.8–50.8% in 2019; 44.9–48.8% in 2020). One-way ANOVA confirmed a significant effect of growth stage on cumulative NH_3 volatilization in both years (2019: $F = 247.85$, $p < 0.001$; 2020: $F = 159.54$, $p < 0.001$). All fertilized treatments showed substantial year-on-year increases in cumulative NH_3 (ranging from 32.6% to 49.6%), whereas the CK increased by only 4.4%.

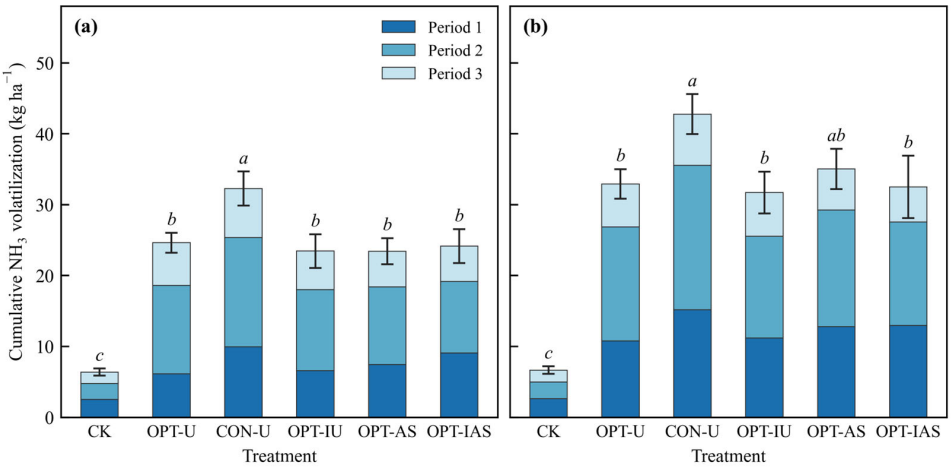

Figure 4. Cumulative NH_3 volatilization (kg ha^{-1}; mean ± SE) by treatment under ambient soil pH in (**a**) 2019 and (**b**) 2020. Stacked bars show contributions from Period 1 (sowing to first irrigation), Period 2 (first to second irrigation, encompassing topdressing), and Period 3 (second irrigation to harvest). Different lowercase letters above bars indicate significant differences among treatments (Duncan's test, $p < 0.05$).

Two-way mixed ANOVA confirmed a significant main effect of soil pH condition on NH_3 volatilization efficiency in both years (Table 2), with no significant Treatment × pH interaction, indicating that the response to pH manipulation was consistent across all fertilizer treatments. An increase of approximately 0.5 pH units above ambient was associated with a 25% increase in volatilization efficiency relative to ambient conditions, whereas a comparable decrease reduced efficiency by up to 18% (Table 3). These responses were directionally consistent across all fertilizer treatments. Under ambient conditions, CON-U exhibited lower volatilization efficiency than the four optimized-rate treatments in both years; this pattern reflects the larger absolute nitrogen denominator in CON-U rather than a reduction in absolute NH_3 losses, as absolute cumulative losses under CON-U were the highest among all treatments. The consistent sensitivity of NH_3 losses to pH variation of less than one unit—at a site where ambient pH already exceeds 8.8—underscores the dominant control exerted by soil alkalinity on NH_3 volatilization in this system.

Table 2. Two-way mixed ANOVA of NH_3 volatilization efficiency in response to fertilizer treatment and soil pH manipulation.

Source	2019	2020
Treatment	$F = 137.17$, $p < 0.001$	$F = 420.47$, $p < 0.001$
pH condition	$F = 117.78$, $p < 0.001$	$F = 82.49$, $p < 0.001$
Treatment × pH	$F = 1.43$, $p = 0.226$	$F = 2.17$, $p = 0.080$

Table 3. NH_3 volatilization efficiency (%) under ambient and pH-adjusted conditions for each treatment in 2019 and 2020 (mean ± SE).

Year	Treatment	Effic. Ambient (%)	Effic. pH^+ (%)	Effic. pH^- (%)
2019	OPT-U	13.67 ± 0.40 a	15.66 ± 0.88	12.51 ± 0.54
	OPT-IU	13.02 ± 1.04 a	16.09 ± 0.15	12.56 ± 1.57
	OPT-AS	13.00 ± 0.51 a	14.64 ± 1.13	11.28 ± 0.47
	OPT-IAS	13.41 ± 0.62 a	16.74 ± 0.09	12.84 ± 0.51
	CON-U	8.06 ± 0.54 b	9.85 ± 0.26	7.16 ± 0.31
2020	OPT-U	18.29 ± 0.91 a	20.09 ± 0.43	17.50 ± 0.28
	OPT-IU	17.61 ± 0.56 a	18.75 ± 0.30	16.10 ± 0.13
	OPT-AS	19.45 ± 0.93 a	22.05 ± 0.51	18.57 ± 0.57
	OPT-IAS	18.05 ± 1.93 ab	19.99 ± 0.50	16.33 ± 0.08
	CON-U	10.69 ± 0.08 b	11.05 ± 0.29	8.81 ± 0.30

Different lowercase letters within each year's ambient column indicate significant differences among treatments (Duncan's test, $p < 0.05$). pH^+: soil pH elevated ~0.5 units relative to ambient; pH^-: soil pH reduced ~0.5 units. Values for pH^+ and pH^- columns represent means ± SE; no between-treatment statistical comparisons were performed for pH-adjusted conditions.

3.2. N_2O Emissions in Response to Nitrogen Rate and Fertilizer Formulation

Cumulative N_2O emissions were associated with both nitrogen application rate and fertilizer formulation (Figure 5). CON-U produced the highest seasonal emissions in both years (1241.4 ± 29.6 and 1560.9 ± 32.0 g ha^{-1} in 2019 and 2020), exceeding OPT-U by more than 129% and CK by eight- to tenfold ($p < 0.05$). Among optimized-rate treatments, OPT-AS consistently generated higher N_2O emissions than OPT-U by approximately 18% in both years ($p < 0.05$). OPT-IU reduced cumulative N_2O emissions relative to OPT-U by approximately 21–24%, and OPT-IAS reduced emissions relative to OPT-AS by approximately 31–32% ($p < 0.05$ for both). The period between the first and second irrigations (Period 2) contributed the largest proportion of seasonal N_2O emissions across fertilized treatments (38–58% in 2019; 42–62% in 2020). One-way ANOVA confirmed a significant effect of growth stage on cumulative N_2O emissions in both years (2019: $F = 1599.03$,

$p < 0.001$; 2020: F = 1727.93, $p < 0.001$). All fertilized treatments exhibited increases in N_2O emissions from 2019 to 2020 (approximately 19–26%), whereas CK showed minimal change.

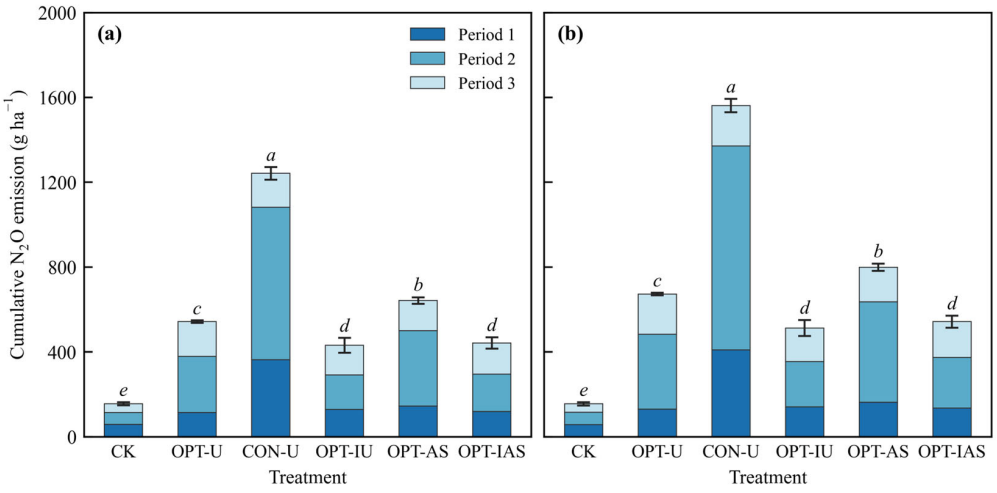

Figure 5. Cumulative N_2O emissions (g ha^{-1}; mean ± SE) by treatment and period in (**a**) 2019 and (**b**) 2020. Different lowercase letters above bars indicate significant differences among treatments (Duncan's test, $p < 0.05$).

3.3. Post-Harvest Soil Mineral Nitrogen Storage

Post-harvest mineral nitrogen storage in the 0–90 cm soil profile differed significantly among treatments in both years (Figure 6), with all fertilized treatments retaining more mineral nitrogen than CK ($p < 0.05$). Total profile storage increased from 2019 to 2020 across all treatments, with increases ranging from 26.7% (CK) to 66.6% (OPT-IU). CON-U retained the highest mineral nitrogen in both years (120.9 ± 0.5 kg ha^{-1} in 2019; 163.9 ± 4.8 kg ha^{-1} in 2020), exceeding OPT-U by 55% and 43%, respectively. Among optimized-rate treatments, total storage in 2019 ranged from 59.0 ± 2.9 kg ha^{-1} (OPT-IU) to 77.8 ± 1.4 kg ha^{-1} (OPT-U), with OPT-AS and OPT-IAS not significantly different from OPT-U in either year ($p > 0.05$). OPT-IU consistently retained less mineral nitrogen than OPT-U in both years ($p < 0.05$), representing the lowest post-harvest soil nitrogen storage among all fertilized treatments and suggesting improved nitrogen capture by the crop under urease inhibition.

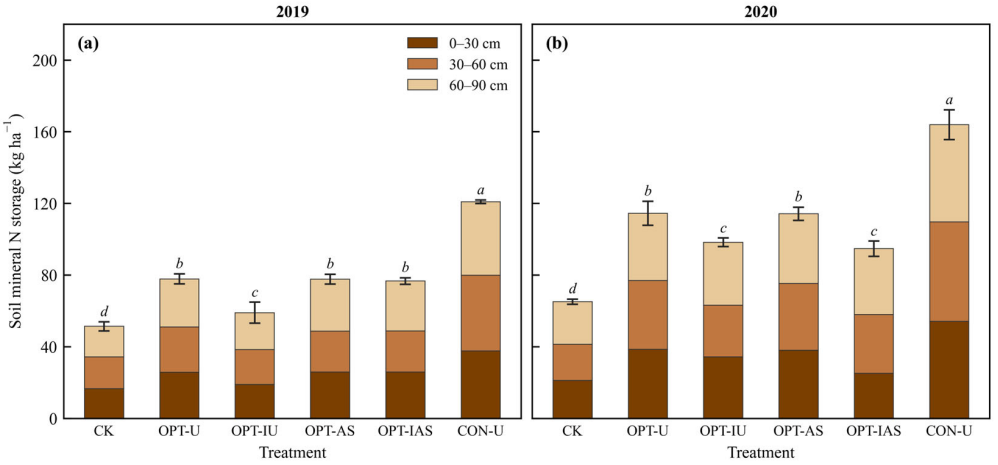

Figure 6. Post-harvest soil mineral nitrogen storage (kg ha^{-1}; mean ± SE) by treatment and depth layer in 2019 (**a**) and 2020 (**b**). Different lowercase letters above bars indicate significant differences among treatments (Duncan's test, $p < 0.05$).

3.4. Grain Yield, Global Warming Potential, and Emission Intensity

Grain yield increased with nitrogen application rate in both years, with CON-U achieving the highest values (11.22 ± 0.45 t ha^{-1} in 2019; 15.03 ± 1.05 t ha^{-1} in 2020) and CK the lowest ($p < 0.05$; Table 4). Among optimized-rate treatments, OPT-IU and OPT-IAS produced significantly higher yields than OPT-U in both years, while OPT-AS showed intermediate values not significantly different from OPT-U in 2019. Differences in GWP among treatments were small in absolute terms, varying by less than 15%, whereas grain yield varied by more than 50%. CON-U was the only treatment with GWP significantly higher than all others in both years ($p < 0.05$), reflecting its substantially greater N_2O emissions. GHGI showed an inverse relationship with yield, with CON-U exhibiting the lowest values in both years (0.300 kg CO_2-eq kg^{-1} in 2019; 0.229 kg CO_2-eq kg^{-1} in 2020) and CK the highest. This outcome reflects the fact that the yield increment achieved under CON-U was proportionally larger than its GWP increment relative to other treatments—a yield-dilution effect on emission intensity—rather than a reduction in absolute N_2O emissions, which were the highest of all treatments. Among optimized-rate treatments, OPT-IU and OPT-IAS achieved lower GHGI than OPT-U ($p < 0.05$), driven primarily by their yield advantage rather than by large differences in GWP.

Table 4. GWP, Grain yield, and GHGI for all treatments in 2019 and 2020 (mean ± SD).

Year	Treatment	GWP (kg CO_2-eq ha^{-1})	Yield (t ha^{-1})	GHGI (kg CO_2-eq kg^{-1})
2019	CK	3065.32 ± 2.04 b	6.51 ± 0.42 d	0.471 ± 0.030 a
	OPT-U	3170.94 ± 1.56 b	7.36 ± 1.02 d	0.431 ± 0.060 b
	OPT-IU	3140.42 ± 9.55 b	9.37 ± 0.13 b	0.335 ± 0.005 d
	OPT-AS	3198.08 ± 4.23 b	8.11 ± 0.91 c	0.394 ± 0.045 c
	OPT-IAS	3143.56 ± 7.26 b	9.53 ± 0.49 b	0.330 ± 0.017 d
	CON-U	3361.90 ± 8.08 a	11.22 ± 0.45 a	0.300 ± 0.012 e
2020	CK	3065.18 ± 2.21 b	8.14 ± 0.57 e	0.377 ± 0.026 a
	OPT-U	3206.38 ± 1.67 b	9.94 ± 0.70 d	0.323 ± 0.023 b
	OPT-IU	3162.75 ± 10.32 b	12.18 ± 0.85 b	0.260 ± 0.018 d
	OPT-AS	3240.91 ± 4.56 b	10.54 ± 0.74 c	0.307 ± 0.022 c
	OPT-IAS	3170.94 ± 7.83 b	12.87 ± 0.90 b	0.246 ± 0.017 d
	CON-U	3449.13 ± 8.74 a	15.03 ± 1.05 a	0.229 ± 0.016 e

Different lowercase letters within the same column indicate significant differences among treatments (Duncan's test, $p < 0.05$).

3.5. Relationships Among Nitrogen Loss Pathways and Yield

Pearson correlation coefficients were computed among nitrogen application rate, cumulative NH_3 volatilization, cumulative N_2O emissions, post-harvest soil mineral nitrogen storage (0–90 cm), and grain yield based on plot-level observations across both years ($n = 48$). Because all response variables share a common dependence on nitrogen application rate, these correlations should be interpreted as descriptive of co-variation across the management gradient rather than as evidence of independent mechanistic associations. Nitrogen application rate showed significant positive correlations with all response variables ($r = 0.686$–0.938, all $p < 0.01$; Figure 7), consistent with its role as the primary driver of co-variation across the management gradient. NH_3 volatilization and N_2O emissions were positively correlated ($r = 0.806$, 95% CI [0.677, 0.887], $p < 0.01$), as were NH_3 volatilization and post-harvest soil nitrogen storage ($r = 0.836$, 95% CI [0.723, 0.905], $p < 0.01$), and N_2O emissions and soil nitrogen storage ($r = 0.906$, 95% CI [0.838, 0.947], $p < 0.01$). Grain yield was positively correlated with NH_3 volatilization ($r = 0.755$, $p < 0.01$), N_2O emissions ($r = 0.689$, $p < 0.01$), and soil nitrogen storage ($r = 0.797$, $p < 0.01$). All correlation patterns

were directionally consistent between 2019 (n = 24) and 2020 (n = 24), indicating that the observed relationships were stable across years and not specific to either growing season.

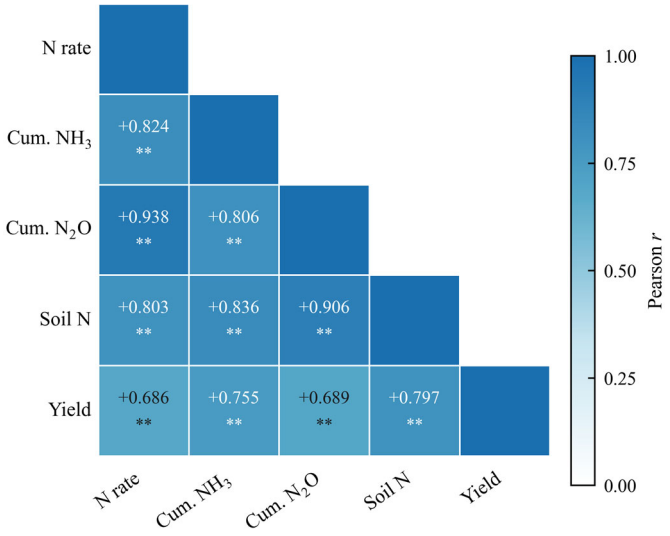

Figure 7. Pearson correlation heatmap among nitrogen application rate (N rate), cumulative NH_3 volatilization (Cum. NH_3), cumulative N_2O emissions (Cum. N_2O), post-harvest soil mineral nitrogen storage (Soil N), and grain yield. Correlations are based on plot-level observations (n = 48). ** $p < 0.01$.

4. Discussion

The results demonstrate that nitrogen application rate was the primary driver of both NH_3 volatilization and N_2O emissions, consistent with its role in elevating soil ammonium concentrations, which simultaneously supply substrate for volatilization and for microbial nitrification–denitrification processes [27,28]. However, the two loss pathways responded differently to fertilizer formulation and inhibitor application, indicating that nitrogen rate alone does not determine their relative magnitudes. NH_3 volatilization was insensitive to fertilizer formulation and inhibitor inclusion, whereas N_2O emissions differed significantly between ammonium sulfate-based and urea-based formulations and were substantially reduced when inhibitors were included. This divergence reflects the fundamental mechanistic distinction between NH_3 volatilization—a physicochemical equilibrium process governed by soil pH and ammonium availability—and N_2O production—a biologically mediated process dependent on nitrifier and denitrifier activity [29]. The insensitivity of NH_3 volatilization to fertilizer formulation is consistent with evidence that the loss difference between urea and ammonium sulfate virtually disappears once soil pH exceeds 7.0, when thermodynamic control of the NH_4^+–NH_3 equilibrium overrides substrate-level effects of fertilizer formulation [30]. Similar decoupling between the two pathways has been documented in northern Chinese cropping systems, where urease and nitrification inhibitors target biochemically distinct steps in the nitrogen transformation sequence, and NH_3 and N_2O responses to the same management inputs consistently diverge [9].

Soil pH exerted a dominant influence on NH_3 volatilization efficiency, overriding the effects of fertilizer formulation and inhibitor application. The microplot pH manipulation experiment demonstrated that a change of only 0.5 pH units at the ambient site pH of ~8.8 altered volatilization efficiency by up to 25% upward and up to 18% downward, relative to ambient conditions. This asymmetric sensitivity is consistent with the nonlinear relationship between pH and the NH_4^+–NH_3 equilibrium, in which the proportion of dissolved ammonium present as volatile NH_3 increases sharply above pH 7.5 [11]. Large-scale data syntheses across Chinese upland crops and Mediterranean calcareous systems

consistently identify soil pH as the most important edaphic variable controlling NH_3 volatilization, surpassing fertilizer type, application method, and crop type in relative importance [31,32], and the within-site, within-season pH manipulation conducted here provides more direct evidence of this relationship under field conditions than cross-site comparisons allow.

The higher N_2O emissions observed under OPT-AS relative to OPT-U at equivalent nitrogen rates are consistent with the immediate availability of NH_4^+ in ammonium sulfate, which enters the nitrification pathway without the hydrolysis step required for urea and may therefore sustain higher rates of ammonia oxidation during the critical post-irrigation period [33]. In alkaline soils, ammonia-oxidizing bacteria (AOB) dominate the nitrification process and are the primary contributors to nitrification-derived N_2O production, with NH_4^+ amendment shown to stimulate AOB activity and N_2O emissions particularly at high pH [34]. In calcareous fluvo-aquic soils of northern China—geochemically comparable to the alkaline irrigated soils of the Hetao District—isotopomeric evidence has demonstrated that NH_4^+-based fertilizer application actively drives O_2 consumption and induces suboxic conditions, under which ammonia oxidation and linked nitrifier denitrification together account for the large majority of total N_2O production [35]. Under transiently anaerobic conditions generated by flood inundation, both nitrifier denitrification and heterotrophic denitrification respond strongly to NH_4^+ substrate availability at low O_2 concentrations [36], providing a plausible mechanistic basis for the elevated N_2O observed under ammonium sulfate. A two-year field experiment in irrigated maize independently found that ammonium sulfate produced the highest cumulative N_2O losses among tested fertilizer types regardless of irrigation system, with DMPP being the most effective mitigation strategy [37], consistent with the pattern observed here. However, as direct measurements of soil O_2 dynamics, nitrification rates, and denitrification rates were not conducted in the present study, the relative contributions of nitrifier denitrification and heterotrophic denitrification to the observed N_2O difference between OPT-AS and OPT-U cannot be quantified, and the pathway attribution remains inferential. Nonetheless, It should be noted that globally, ammonium sulfate does not consistently produce higher N_2O than urea, and the reverse pattern has been reported in several field studies under different irrigation and pH regimes [38]; the elevated emissions under OPT-AS are therefore likely context-specific, reflecting the rapid post-irrigation oxygen depletion and high ambient pH characteristic of flood-irrigated alkaline soils in the Hetao District.

Irrespective of fertilizer type, the pronounced concentration of N_2O emissions in Period 2—encompassing topdressing and the first flood irrigation event—across all fertilized treatments is consistent with transient anaerobic conditions generated by flood inundation, which intensify denitrification during a narrow post-irrigation window [39]. Mechanistic evidence confirms that transient anoxia stimulates denitrification capacity and reduces the N_2O-to-N_2 reduction ratio, producing short-lived but intense N_2O pulses that account for a disproportionate share of seasonal emissions [40]. OPT-IAS reduced N_2O emissions by 31–32% without increasing NH_3 volatilization, contrasting with the global meta-analytic finding that nitrification inhibitors increase NH_3 emissions by an average of 35.7%, particularly in alkaline soils. This discrepancy likely reflects the dominant thermodynamic control of soil pH on the NH_4^+–NH_3 equilibrium established above: at pH > 8.8, any secondary effect of DMPP on ammonium substrate availability is masked, consistent with the observation that the NH_3 penalty of nitrification inhibitor application is amplified at lower pH where substrate-level effects become relatively more important [8]. OPT-IU similarly showed no increase in NH_3 volatilization, consistent with the mechanism of NBPT action: delayed urea hydrolysis reduces the transient peak in NH_4^+ concentration at the soil surface, which, at strongly alkaline pH, is the primary determinant of volatilization

flux [41]. The reduction in post-harvest soil mineral nitrogen under OPT-IU relative to OPT-U in both years further suggests that NBPT-mediated slowing of urea hydrolysis improved the synchrony between nitrogen supply and crop demand, reducing residual nitrogen accumulation susceptible to subsequent loss [42].

The inverse relationship between GHGI and grain yield across treatments—most pronounced for CON-U, which achieved the lowest GHGI despite the highest absolute N_2O emissions—illustrates a well-recognized limitation of emission intensity metrics as standalone environmental indicators [43]. This yield-dilution effect is pervasive across global maize, wheat, and rice systems: yield-scaled N_2O emissions decline mechanically as yields increase beyond system-specific thresholds, such that high-yielding treatments appear environmentally favorable even when their absolute emission loads are highest [44,45]. The yield-dilution effect under CON-U obscures its substantially greater absolute gaseous losses and post-harvest soil nitrogen accumulation (up to 163.9 kg N ha^{-1} in 2020), which represents a legacy nitrogen pool at risk of leaching or denitrification in subsequent seasons. Comprehensive evaluation of nitrogen management strategies, therefore, requires simultaneous consideration of absolute emission loads, residual soil nitrogen, and emission intensity rather than reliance on any single metric. Among optimized-rate treatments, OPT-IU and OPT-IAS achieved the most favorable combination of outcomes—higher grain yield, lower N_2O emissions, lower GHGI, and in the case of OPT-IU, reduced residual soil nitrogen—relative to OPT-U, without increasing NH_3 volatilization. However, as the preceding analysis shows, no single modification was sufficient to address all nitrogen loss pathways simultaneously.

The present study offers several methodological strengths: the simultaneous quantification of NH_3 volatilization, N_2O emissions, and post-harvest soil mineral nitrogen storage within a single replicated field experiment enables direct evaluation of trade-offs among competing nitrogen loss pathways, rather than inference from separate studies conducted under different conditions; the embedded soil pH manipulation sub-experiment provides within-site, within-season evidence of pH control on NH_3 volatilization efficiency, free from the confounding by soil type, climate, and management history inherent in cross-site comparisons; and the two-year design, with consistent treatment rankings across contrasting climatic seasons, establishes temporal robustness beyond what single-year studies can support. Several limitations should nonetheless be acknowledged. The experimental design was not fully factorial with respect to fertilizer type and inhibitor type—NBPT was applied exclusively with urea (OPT-IU) and DMPP exclusively with ammonium sulfate (OPT-IAS), reflecting commercially available inhibitor–fertilizer pairings in the study region—and the independent contributions of these two factors to the observed differences in N_2O emissions therefore cannot be fully disentangled; the comparisons are best interpreted as evaluations of fertilizer formulation effects under conditions representative of regional agricultural practice. The study was additionally conducted at a single experimental site within the Hetao Irrigation District; while the site conditions—alkaline soil pH, high nitrogen inputs, and seasonal flood irrigation—are broadly representative of the district, direct extrapolation of quantitative emission magnitudes to systems differing in soil texture, organic matter content, or irrigation regime should be made with caution. The two-year observation period, while sufficient to establish cross-year consistency in treatment rankings, does not capture the longer-term dynamics of residual soil nitrogen accumulation that may develop under sustained application of the evaluated management strategies. At the system level, a fundamental constraint is the pollution swapping characteristic of alkaline irrigated conditions [46]: NH_3 volatilization remained governed by soil pH and nitrogen input irrespective of fertilizer formulation or inhibitor application, whereas N_2O reductions were achievable through inhibitor use, and trade-off analyses indicate

that inhibitor-induced NH_3 increases can under some conditions offset the climate benefit of N_2O reduction [47]. Achieving concurrent mitigation of both pathways will therefore require complementary interventions—such as deep placement or drip fertigation, which have been shown to simultaneously reduce NH_3, N_2O, and NO_3^- leaching in alkaline Chinese cropping systems [9,48]—beyond rate optimization and inhibitor application alone.

5. Conclusions

This two-year field study demonstrated that NH_3 volatilization and N_2O emissions are governed by distinct controlling factors in alkaline, flood-irrigated maize systems. NH_3 volatilization was primarily determined by nitrogen application rate and soil pH; a 0.5-unit increase in soil pH above the ambient value of ~8.8 elevated volatilization efficiency by up to 25% relative to ambient, while fertilizer formulation and inhibitor inclusion produced no significant effect on cumulative losses. N_2O emissions were more sensitive to fertilizer formulation and were reduced by approximately 21–32% under inhibitor inclusion without a compensatory increase in NH_3 volatilization. These contrasting responses indicate that the two gaseous loss pathways are subject to distinct regulatory controls beyond their shared dependence on nitrogen input.

Among the evaluated strategies, optimized nitrogen management combined with inhibitor application (OPT-IU and OPT-IAS) achieved the most favorable balance of outcomes: higher grain yields, lower N_2O emissions, lower GHGI, and reduced residual soil nitrogen accumulation relative to urea alone at equivalent nitrogen rates. However, NH_3 losses remained governed by soil alkalinity irrespective of fertilizer formulation, indicating that concurrent mitigation of both gaseous loss pathways in alkaline flood-irrigated systems will require additional interventions targeting nitrogen delivery, beyond inhibitor application and rate optimization alone.

Author Contributions: Conceptualization, Y.G.; methodology, Y.G. and H.Y.; software, Y.G. and Y.T.; validation, H.Y. and W.Z.; formal analysis, Y.G., Y.D. and W.Z.; investigation, Y.D., H.Y., Y.T. and W.Z.; resources, F.L.; data curation, Y.T. and W.Z.; writing—original draft preparation, Y.G.; writing—review and editing, Y.G., Y.H. and F.L.; supervision, Y.H. and F.L.; project administration, F.L.; funding acquisition, F.L. All authors have read and agreed to the published version of the manuscript.

Funding: This research was funded by the National Key Research and Development Program of China, grant number 2018YFD0800802.

Institutional Review Board Statement: Not applicable.

Informed Consent Statement: Not applicable.

Data Availability Statement: Data are contained within the article.

Conflicts of Interest: The authors declare no conflicts of interest.

Abbreviations

The following abbreviations are used in this manuscript:

EEF	Enhanced-efficiency fertilizer
NBPT	N-(n-butyl) thiophosphoric triamide
DMPP	3,4-dimethylpyrazole phosphate
GWP	Global warming potential
GHGI	Greenhouse gas emission intensity
OPT-U	Optimized nitrogen rate urea
CON-U	Conventional nitrogen rate urea
OPT-IU	Optimized nitrogen rate urea + NBPT
OPT-AS	Optimized nitrogen rate ammonium sulfate

OPT-IAS	Optimized nitrogen rate ammonium sulfate + DMPP
CK	Control check
UI	Urease inhibitor
NI	Nitrification inhibitor

References

1. Liu, L.; Xu, W.; Lu, X.; Zhong, B.; Guo, Y.; Lu, X.; Zhao, Y.; He, W. Exploring global changes in agricultural ammonia emissions and their contribution to nitrogen deposition since 1980. *Proc. Natl. Acad. Sci. USA* **2022**, *119*, e2121998119. [CrossRef]
2. Pan, B.; Lam, S.K.; Mosier, A.; Luo, Y.; Chen, D. Ammonia volatilization from synthetic fertilizers and its mitigation strategies: A global synthesis. *Agric. Ecosyst. Environ.* **2016**, *232*, 283–289. [CrossRef]
3. Galloway, J.N.; Townsend, A.R.; Erisman, J.W.; Bekunda, M.; Cai, Z.; Freney, J.R.; Martinelli, L.A.; Seitzinger, S.P.; Sutton, M.A. Transformation of the nitrogen cycle: Recent trends, questions, and potential solutions. *Science* **2008**, *320*, 889–892. [CrossRef]
4. Fowler, D.; Coyle, M.; Skiba, U.; Sutton, M.A.; Cape, J.N.; Reis, S.; Sheppard, L.J.; Jenkins, A.; Grizzetti, B.; Galloway, J.N.; et al. The global nitrogen cycle in the twenty-first century. *Philos. Trans. R. Soc. B Biol. Sci.* **2013**, *368*, 20130164. [CrossRef] [PubMed]
5. Canadell, J.G.; Monteiro, P.M.S.; Costa, M.H.; Cotrim Da Cunha, L.; Cox, P.M.; Eliseev, A.V.; Henson, S.; Ishii, M.; Jaccard, S.; Koven, C.; et al. *Global Carbon and Other Biogeochemical Cycles and Feedbacks*; Chapter 5; HAL: Lyon/Villeurbanne, France, 2021.
6. Butterbach-Bahl, K.; Baggs, E.M.; Dannenmann, M.; Kiese, R.; Zechmeister-Boltenstern, S. Nitrous oxide emissions from soils: How well do we understand the processes and their controls? *Philos. Trans. R. Soc. B Biol. Sci.* **2013**, *368*, 20130122. [CrossRef]
7. Tian, H.; Pan, N.; Thompson, R.L.; Canadell, J.G.; Suntharalingam, P.; Regnier, P.; Davidson, E.A.; Prather, M.; Ciais, P.; Muntean, M.; et al. Global nitrous oxide budget (1980–2020). *Earth Syst. Sci. Data* **2024**, *16*, 2543–2604. [CrossRef]
8. Wu, D.; Zhang, Y.; Dong, G.; Du, Z.; Wu, W.; Chadwick, D.; Bol, R. The importance of ammonia volatilization in estimating the efficacy of nitrification inhibitors to reduce N2O emissions: A global meta-analysis. *Environ. Pollut.* **2021**, *271*, 116365. [CrossRef]
9. Zhang, C.; Song, X.; Zhang, Y.; Wang, D.; Rees, R.M.; Ju, X. Using nitrification inhibitors and deep placement to tackle the trade-offs between NH_3 and N_2O emissions in global croplands. *Glob. Change Biol.* **2022**, *28*, 4409–4422. [CrossRef] [PubMed]
10. Sommer, S.G.; Schjoerring, J.K.; Denmead, O.T. Ammonia Emission from Mineral Fertilizers and Fertilized Crops. *Adv. Agron.* **2004**, *82*, 557–622.
11. Zhang, X.; Davidson, E.A.; Mauzerall, D.L.; Searchinger, T.D.; Dumas, P.; Shen, Y. Managing nitrogen for sustainable development. *Nature* **2015**, *528*, 51–59. [CrossRef] [PubMed]
12. Silva, A.G.; Sequeira, C.H.; Sermarini, R.A.; Otto, R. Urease inhibitor NBPT on ammonia volatilization and crop productivity: A meta-analysis. *Agron. J.* **2017**, *109*, 1–13. [CrossRef]
13. Matse, D.T.; Krol, D.J.; Richards, K.G.; Danaher, M.; Cummins, E.; Wang, X.; Forrestal, P.J. Field efficacy of urease inhibitors for mitigation of ammonia emissions in agricultural field settings: A systematic review. *Front. Environ. Sci.* **2024**, *12*, 1462098.
14. Fan, D.; He, W.; Smith, W.N.; Drury, C.F.; Jiang, R.; Grant, B.B.; Shi, Y.; Song, D.; Chen, Y.; Wang, X.; et al. Global evaluation of inhibitor impacts on ammonia and nitrous oxide emissions from agricultural soils: A meta-analysis. *Glob. Change Biol.* **2022**, *28*, 5121–5141. [CrossRef]
15. Tufail, M.A.; Irfan, M.; Umar, W.; Wakeel, A.; Schmitz, R.A. Mediation of gaseous emissions and improving plant productivity by DCD and DMPP nitrification inhibitors: Meta-analysis of last three decades. *Environ. Sci. Pollut. Res.* **2023**, *30*, 64719–64735. [CrossRef] [PubMed]
16. Chen, Y.; Zhao, N.; Hao, Y.; Li, X.; Fan, M.; Shi, X.; Jia, L. Optimizing nutrient inputs by balancing spring wheat yield and environmental effects in the Hetao Irrigation District of China. *Sci. Rep.* **2022**, *12*, 22524. [CrossRef]
17. Li, C.; Xiong, Y.; Cui, Z.; Huang, Q.; Xu, X.; Han, W.; Huang, G. Effect of irrigation and fertilization regimes on grain yield, water and nitrogen productivity of mulching cultivated maize (*Zea mays* L.) in the Hetao Irrigation District of China. *Agric. Water Manag.* **2020**, *232*, 106065. [CrossRef]
18. Ju, X.T.; Xing, G.X.; Chen, X.P.; Zhang, S.L.; Zhang, L.J.; Liu, X.J.; Cui, Z.L.; Yin, B.; Christie, P.; Zhu, Z.L.; et al. Reducing environmental risk by improving N management in intensive Chinese agricultural systems. *Proc. Natl. Acad. Sci. USA* **2009**, *106*, 3041–3046. [CrossRef]
19. Cui, Z.; Wang, G.; Yue, S.; Wu, L.; Zhang, W.; Zhang, F.; Chen, X. Closing the N-use efficiency gap to achieve food and environmental security. *Environ. Sci. Technol.* **2014**, *48*, 5780–5787. [CrossRef]
20. Zhou, J.; Gu, B.; Schlesinger, W.H.; Ju, X. Significant accumulation of nitrate in Chinese semi-humid croplands. *Sci. Rep.* **2016**, *6*, 25088. [CrossRef]
21. Ma, R.; Yu, K.; Xiao, S.; Liu, S.; Ciais, P.; Zou, J. Data-driven estimates of fertilizer-induced soil NH_3, NO and N_2O emissions from croplands in China and their climate change impacts. *Glob. Change Biol.* **2022**, *28*, 1008–1022. [CrossRef] [PubMed]
22. Liu, H.; Li, Y. Dynamics of soil salt and nitrogen and maize responses to nitrogen application in hetao irrigation district, China. *J. Soil Sci. Plant Nutr.* **2022**, *22*, 1520–1533. [CrossRef]

23. Jia, M.; Lapen, D.R.; Su, D.; Mayer, K.U. Multi-domain reactive transport modeling of GHG emissions from macroporous agricultural soils with a focus on N_2O hotspots and hot moments. *Water Resour. Res.* **2025**, *61*, e2025WR040588. [CrossRef]
24. Li, Z.; Guan, K.; Zhou, W.; Peng, B.; Nafziger, E.D.; Grant, R.F.; Jin, Z.; Tang, J.; Margenot, A.J.; Lee, D.; et al. Comparing continuous-corn and soybean-corn rotation cropping systems in the U.S. central Midwest: Trade-offs among crop yield, nutrient losses, and change in soil organic carbon. *Agric. Ecosyst. Environ.* **2025**, *393*, 109739. [CrossRef]
25. Bao, S.D. *Soil Agricultural Chemistry Analysis*, 3rd ed.; China Agriculture Press: Beijing, China, 2000.
26. Wang, Z.; Liu, X.; Ju, X.; Zhang, F. Field in situ determination of ammonia volatilization from soil: Venting method. *J. Plant Nutr. Fertil.* **2002**, *8*, 205–209.
27. Li, C.; Xiong, Y.; Huang, Q.; Xu, X.; Huang, G. Impact of irrigation and fertilization regimes on greenhouse gas emissions from soil of mulching cultivated maize (*Zea mays* L.) field in the upper reaches of Yellow River, China. *J. Clean. Prod.* **2020**, *259*, 120873. [CrossRef]
28. Shcherbak, I.; Millar, N.; Robertson, G.P. Global metaanalysis of the nonlinear response of soil nitrous oxide (N_2O) emissions to fertilizer nitrogen. *Proc. Natl. Acad. Sci. USA* **2014**, *111*, 9199–9204. [CrossRef]
29. Sha, Z.; Ma, X.; Loick, N.; Lv, T.; Cardenas, L.M.; Ma, Y.; Liu, X.; Misselbrook, T. Nitrogen stabilizers mitigate reactive N and greenhouse gas emissions from an arable soil in North China Plain: Field and laboratory investigation. *J. Clean. Prod.* **2020**, *258*, 121025. [CrossRef]
30. Powlson, D.S.; Dawson, C.J. Use of ammonium sulphate as a sulphur fertilizer: Implications for ammonia volatilization. *Soil Use Manag.* **2022**, *38*, 622–634. [CrossRef]
31. Sha, Z.; Ma, X.; Liu, H.; Wang, J.; Lv, T.; Goulding, K.; Liu, X. Crop-specific ammonia volatilization rates and key influencing factors in the upland of China–A data synthesis. *J. Environ. Manag.* **2023**, *336*, 117676. [CrossRef]
32. Hurtado, J.; Velázquez, E.; Lassaletta, L.; Guardia, G.; Aguilera, E.; Sanz-Cobena, A. Drivers of ammonia volatilization in Mediterranean climate cropping systems. *Environ. Pollut.* **2024**, *341*, 122814. [CrossRef]
33. Tian, D.; Zhang, Y.; Mu, Y.; Liu, J.; He, K. Effect of N fertilizer types on N_2O and NO emissions under drip fertigation from an agricultural field in the North China Plain. *Sci. Total Environ.* **2020**, *715*, 136903. [CrossRef]
34. Hu, L.; Dong, Z.; Wang, Z.; Xiao, L.; Zhu, B. The contributions of ammonia oxidizing bacteria and archaea to nitrification-dependent N_2O emission in alkaline and neutral purple soils. *Sci. Rep.* **2022**, *12*, 19928. [CrossRef]
35. Huang, T.; Gao, B.; Hu, X.K.; Lu, X.; Well, R.; Christie, P.; Bakken, L.R.; Ju, X.T. Ammonia-oxidation as an engine to generate nitrous oxide in an intensively managed calcareous Fluvo-aquic soil. *Sci. Rep.* **2014**, *4*, 3950. [CrossRef]
36. Zhu, X.; Burger, M.; Doane, T.A.; Horwath, W.R. Ammonia oxidation pathways and nitrifier denitrification are significant sources of N_2O and NO under low oxygen availability. *Proc. Natl. Acad. Sci. USA* **2013**, *110*, 6328–6333. [CrossRef]
37. Guardia, G.; García-Gutiérrez, S.; Vallejo, A.; Ibáñez, M.A.; Sanchez-Martin, L.; Montoya, M. Nitrous oxide emissions and N-cycling gene abundances in a drip-fertigated (surface versus subsurface) maize crop with different N sources. *Biol. Fertil. Soils* **2024**, *60*, 375–391. [CrossRef]
38. Luo, J.; van der Weerden, T.; Saggar, S.; Di, H.J.; Podolyan, A.; Adhikari, K.; Ding, K.; Lindsey, S.; Luo, D.; Ouyang, L.; et al. Nitrous oxide emission factors for fertiliser ammonium sulphate, diammonium phosphate, and urea. *N. Z. J. Agric. Res.* **2025**, *68*, 569–591. [CrossRef]
39. Ning, D.; Zhang, Y.; Qin, A.; Gao, Y.; Duan, A.; Zhang, J.; Liu, Z.; Zhao, B.; Liu, Z. Interactive effects of irrigation system and level on grain yield, crop water use, and greenhouse gas emissions of summer maize in North China Plain. *Sci. Total Environ.* **2023**, *864*, 161165. [CrossRef]
40. Zhuang, S.; Ding, J.; Lin, W.; Zheng, Q.; Kou, X.; Li, Q.; Xu, C.; Mao, L.; Pan, Y.; Gao, Y.; et al. Transient anoxic conditions boost N_2O emissions by stimulating denitrification capacity and decreasing N_2O reduction ratio in soils with different carbon substrates. *Soil Biol. Biochem.* **2024**, *192*, 109351. [CrossRef]
41. Krol, D.J.; Forrestal, P.J.; Wall, D.; Lanigan, G.J.; Sanz-Gomez, J.; Richards, K.G. Nitrogen fertilisers with urease inhibitors reduce nitrous oxide and ammonia losses, while retaining yield in temperate grassland. *Sci. Total Environ.* **2020**, *725*, 138329. [CrossRef]
42. Liu, G.; Yang, Z.; Du, J.; He, A.; Yang, H.; Xue, G.; Yu, C.; Zhang, Y. Adding NBPT to urea increases N use efficiency of maize and decreases the abundance of N-cycling soil microbes under reduced fertilizer-N rate on the North China Plain. *PLoS ONE* **2020**, *15*, e0240925. [CrossRef]
43. Van Groenigen, J.W.; Velthof, G.L.; Oenema, O.; Van Groenigen, K.J.; Van Kessel, C. Towards an agronomic assessment of N_2O emissions: A case study for arable crops. *Eur. J. Soil Sci.* **2010**, *61*, 903–913. [CrossRef]
44. Kim, D.G.; Giltrap, D.; Sapkota, T.B. Understanding response of yield-scaled N_2O emissions to nitrogen input: Data synthesis and introducing new concepts of background yield-scaled N_2O emissions and N_2O emission-yield curve. *Field Crops Res.* **2023**, *290*, 108737. [CrossRef]
45. Yao, Z.; Guo, H.; Wang, Y.; Zhan, Y.; Zhang, T.; Wang, R.; Zheng, X.; Butterbach-Bahl, K. A global meta-analysis of yield-scaled N_2O emissions and its mitigation efforts for maize, wheat, and rice. *Glob. Change Biol.* **2024**, *30*, e17177. [CrossRef]

46. Stevens, C.J.; Quinton, J.N. Diffuse pollution swapping in arable agricultural systems. *Crit. Rev. Environ. Sci. Technol.* **2009**, *39*, 478–520. [CrossRef]
47. Luo, L.; Cohan, D.S.; Gurung, R.B.; Venterea, R.T.; Ran, L.; Benson, V.; Yuan, Y. Impacts assessment of nitrification inhibitors on US agricultural emissions of reactive nitrogen gases. *J. Environ. Manag.* **2024**, *359*, 121043. [CrossRef]
48. Zheng, J.; Zhou, M.; Zhu, B.; Fan, J.; Lin, H.; Ren, B.; Zhang, F. Drip fertigation sustains crop productivity while mitigating reactive nitrogen losses in Chinese agricultural systems: Evidence from a meta-analysis. *Sci. Total Environ.* **2023**, *886*, 163804. [CrossRef]

Disclaimer/Publisher's Note: The statements, opinions and data contained in all publications are solely those of the individual author(s) and contributor(s) and not of MDPI and/or the editor(s). MDPI and/or the editor(s) disclaim responsibility for any injury to people or property resulting from any ideas, methods, instructions or products referred to in the content.